Partitioning water source and sinking process of a groundwater-dependent desert plant community

Ran Liu, Yugang Wang, Congjuan Li, Jie Ma & Yan Li

Plant and Soil
An International Journal on Plant-Soil Relationships

ISSN 0032-079X
Volume 430
Combined 1-2

Plant Soil (2018) 430:73-85
DOI 10.1007/s11104-018-3714-6

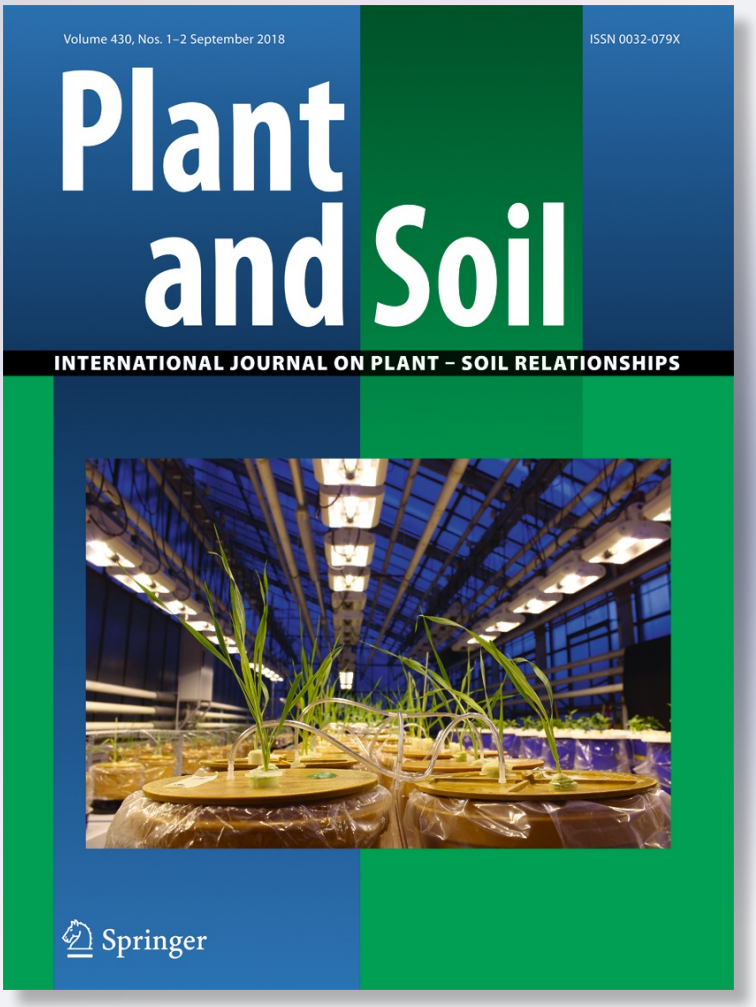

Springer

Plant Soil (2018) 430:73–85
https://doi.org/10.1007/s11104-018-3714-6

REGULAR ARTICLE

Partitioning water source and sinking process of a groundwater-dependent desert plant community

Ran Liu · Yugang Wang · Congjuan Li · Jie Ma · Yan Li

Received: 6 February 2018 / Accepted: 11 June 2018 / Published online: 21 June 2018

Abstract

Background and aims Desert plant community is often structured in two distinct layers of woody and herbaceous plants. Partitioning its water source and sinking process remains a key uncertainty in this water-limited ecosystem. Our aims are to partition the evapotranspiration (ET) components into water loss from bare soil, shrub, and herbaceous plants; estimate the contributions of groundwater to ET and shrub layer transpiration (T_{shrub}); and determine the major drivers of ET components in a groundwater-dependent desert plant community in Central Asia.

Methods Eddy covariance, static chambers, and microlysimeters were used to measure ET and its components (transpiration and evaporation). Oxygen stable isotope and IsoSource model were used to determine the water source of dominant shrubs (*Haloxylon ammodendron*).

Results The seasonal pattern of transpiration (T) for the herbaceous layer (T_{herb}) differed markedly from that for T_{shrub}. T_{herb} reached the maximum values at the beginning of the growing season, and then decreased to nearly zero at the middle and end of the growing seasons. Conversely, T_{shurb} were able to maintain throughout the growing season due to the deep root access to groundwater. In total, T_{shrub}, T_{herb}, and evaporation (E) were 70, 16, and 82 mm year^{-1}, they account for 42, 9, and 49% of total ET during 2014. Most of the groundwater was consumed by T_{shrub} (51 mm year^{-1}), accounted for 73% of T_{shrub}. The contribution of groundwater to ET was 60 mm year^{-1}, representing more than 35% of total ET during 2014. The seasonal dynamics of T_{shrub}, T_{herb}, and E were shaped by different drivers: T_{shrub}: air temperature; T_{herb}: soil water content and herbaceous plant cover; E: net radiation and precipitation.

Conclusions This study demonstrated that a better understanding of the source and sinking process of ET is crucial for predicting hydrological response under ongoing and projected climatic change scenarios in a groundwater-dependent desert plant community.

Keywords Desert ecosystem · Evaporation · Groundwater · Transpiration · Vegetation components

Responsible Editor: Susan Schwinning.

R. Liu · Y. Wang · J. Ma · Y. Li (✉)
State Key Lab of Desert and Oasis Ecology, Xinjiang Institute of Ecology and Geography, Chinese Academy of Sciences, 818 South Beijing Road, Urumqi 830011 Xinjiang, China
e-mail: liyan@ms.xjb.ac.cn

C. Li
National Engineering Technology Research Center for Desert-Oasis Ecological Construction, Xinjiang Institute of Ecology and Geography, Chinese Academy of Sciences, 818 South Beijing Road, Urumqi 830011 Xinjiang, China

Introduction

Evapotranspiration (ET) is the largest component of the terrestrial water balance after precipitation (Morillas et al. 2013). It emphasizes the combined source associated with two different components: evaporation from wet surfaces (E) and transpiration through plants (T)

(Law et al. 2002; Anderson et al. 2008; Schlesinger and Jasechko 2014). To partition ET into *E* and *T* and investigate the factors controlling ET components is one of the most important ecohydrological challenges and it has significant implications for water budgets and also for biogeochemical mechanisms that determine ecosystem function and structure (Austin et al. 2004; Wang et al. 2015). Although ET has been widely measured (e.g., FLUXNET), its partitioning into *E* and *T* is still subject to debate and it has been challenging to identify and quantify them in the field (Huxman et al. 2005; Jasechko et al. 2013; Sutanto et al. 2014).

In water-limited ecosystems, the plant communities are often structured in two distinct layers of woody and herbaceous plants (Lloyd et al. 2008; Vourlitis et al. 2015; De Arruda et al. 2016). Partitioning ET into *E* and *T* is not a simple task since these systems composed of two quite different plant life forms (Joffre and Rambal 1993; Baldocchi and Xu 2007). Furthermore, the different life forms are quite variable regarding water use, with deep-rooted woody plants and shallow-rooted herbaceous plants (Huxman et al. 2004). Understanding how these different components control water transfer to the atmosphere (via *T*) and partitioning ET into different components are particularly critical as climate change and vegetation dynamics may have unexpected impacts on these systems (Huxman et al. 2005; Wang et al. 2014). A recent analysis found that ET partitioning varies with woody plant cover due to their effect on *T* per unit leaf area and not due to differences in *E* (Villegas et al. 2015). Liu et al. (2012) found that herbaceous plant cover strongly affected water budget in a phreatophyte-dominated desert ecosystem. Despite the fact that different plant components can regulate ET, we still lack a solid understanding of the consequences of these potentially important controls on the fundamental coupling of ET.

Groundwater uptake by phreatophyte can be a major water resource of ET, and is a significant part of the water budget in water-limited ecosystems (Fitzpatrick et al. 2001; Scott et al. 2008, 2014; Connor et al. 2013). In recent years, studies focused on quantification groundwater uptake by plants has increased; using remote sensing, eddy covariance, sap flow technique, water table fluctuation method, groundwater modeling, and stable isotopes analysis (Fahle and Dietrich 2014; Kool et al. 2014; Emus et al. 2015; Balugani et al. 2017). Miller et al. (2010) using the water table fluctuation method in an oak savanna, their results showed that groundwater uptake contributed up to 90% of total ET during the dry season. Barbeta and Penuelas (2017) presents an example using stable isotopes and mixing models to quantify the relative contribution of groundwater to plant transpiration; they defined that plant use of groundwater represented on average 49% in dry seasons and 28% in wet seasons. A better understanding of how groundwater uptake by plants contributes to ET and its components are needed, particularly under projected climatic change scenarios in water-limited ecosystems associated with groundwater table fluctuations. More specifically, improved representation of ET resource derived from groundwater will improve understanding and modeling of large-scale ecological, hydrological, and atmospheric processes.

The Gurbantonggut Desert is the second largest desert in China. Its vegetation community composition is divided into woody (referred to as "shrub" below) and herbaceous layers (Li et al. 2013). The herbaceous layer is composed of spring annuals, summer annuals, and perennials, all of which use PPT as the main water resource (Huang and Li 2015). The shrub layer is dominated by phreatophytes (which depend primarily on groundwater) and respond in a non-linear fashion to growing season precipitation (Elmore et al. 2006; Dai et al. 2015). This typical "two-layer" structure and diversified water-use strategies by different plant life forms allow the assessment of partition source of ET, originating from bare soil, shrub, and herbaceous layers, respectively, and estimating the contribution of groundwater to ET and its components in a groundwater-dependent desert plant community. This study uses a combination of eddy covariance (EC), static chambers, micro-lysimeters, and oxygen stable isotope measurements to (1) define the seasonal patterns in ET components by bare soil, shrub and herbaceous layers; (2) assess the contributions of groundwater to ET and its components; and (3) determine the major drivers of ET components.

To meet these objectives, we will evaluate two hypotheses: firstly, seasonal patterns and main drivers of each ET components would differ, as shrub and herbaceous plants have different phenology and rooting depth (Bertram and Dewar 2013). Secondly, groundwater is a relevant part to the total water balance in these desert ecosystems, as dominated shrub plants depend on groundwater as the primary water source (Dai et al. 2015). This study aimed to increase our understanding to water budget in groundwater-dependent desert plant

community, which will result in better predictions of these processes under ongoing and projected climatic change scenarios.

Materials and methods

Site description

This study was carried out at the southern periphery of the Gurbantonggut Desert in Central Asia (44° 17′ N, 87° 56′ E, 475 m a.s.l). This region has a continental arid temperate climate, with a hot, dry summer and a cold winter. The air temperature ranges from a minimum of − 42.2 °C in winter to a maximum of 44.2 °C in summer, and the annual mean temperature is 6.6 °C. Annual mean precipitation is 163 mm, around 75% of which falls in the growing season (May–October). Precipitation prior the growing season (November–April) is mostly in the form of snow, which covers the soil for most of this period and melts in April (Zhou et al. 2012). Soils are desert solonetz in 0–100 cm, with eolian sandy soil at the top. The water table fluctuates between 3- and 5-m depths. The water table change has yearly amplitude of 1 m, shallowest at the end of spring (May–June), which is recharged by snowmelt runoff from the Tianshan Mountains, and then getting deeper when the dry summer begins. The plant community is dominated by the deep-rooted desert shrub *Haloxylon ammodendron*, which depends on groundwater to survive (Dai et al. 2015). Even when the water table goes down (such as summer period), the soil at that depth was still wet for years; thus, fluctuation of groundwater at this scale would not affect water supply to the deep-rooted desert shrubs. The shallow-rooted herbaceous component of the community can be divided into two groups: spring annuals, and summer annuals and perennials. The spring annuals generally use snowmelt water and spring precipitation to grow, and they are dominated by *Alyssum linifolium*, *Schismus arabicus*, *Lactuca undulata*, and *Erodium oxyrrhynchum* (Fan et al. 2013; Huang and Li 2015). Summer annuals and perennials (including *Salsola nitraria*, *Suaeda salsa*, *Salicornia europaea*, and *Ceratocarpus arenarius*) use summer precipitation as the main source of water. In this study, the growing season (May–October) was divided into 60-day blocks representing the beginning (May–June; when the community is dominated by shrubs and spring annuals), middle (July–August; dominated by shrubs, summer annuals and perennials), and the end of the growing season (September–October; dominated by shrubs) (Liu et al. 2016).

Eddy covariance

EC measurements have been conducted at the site since 2010. The system consisted of a 3-D ultrasonic anemometer-thermometer (STA-5055, KAIJO Corporation, Tokyo, Japan) and an open-path infrared gas (CO_2/H_2O) analyzer (LI-7500, LI-COR Inc., Lincoln, NE, USA) at a height of 3 m. The former measures instantaneous fluctuations of the horizontal, vertical, and lateral wind speed and the virtual temperature (T_a), while the latter measures instantaneous fluctuations in the concentrations of CO_2 and water vapor. The data were measured at 10 Hz, and logged with a CR23X data-logger (Campbell Scientific Inc., Logan, UT, USA). Additional meteorological instruments measured air temperature and humidity (MP300, Campbell Scientific Ltd., Shepshed, UK), soil temperature (107 L, Campbell Scientific Inc., Logan), photosynthetic active radiation (LI-190SB, LI-COR Inc.), and net radiation (CNR4, Kipp & Zonen). Two soil heat flux plates (HFP01SC, Hukseflux, The Netherlands) installed 5 cm below the soil surface measured soil heat flux. These data were logged with a CR23X data-logger (Campbell Scientific Inc., Logan, UT, USA). Hourly measurements of volumetric soil water content integrated over 0–30 cm were made at beneath shrubs and interplant spaces (ECH_2O probes, Decagon Devices, Pullman, WA, USA) during the 2014 growing season.

The software EdiRe (www.geos.ed.ac.uk/abs/research/micromet/EdiRe: developed by the University of Edinburgh, UK) was used to calculate eddy fluxes using the following standard corrections: spike removal, planar rotation (Wilczak et al. 2001), auto-detection of the time delay between different sensors, spectral correction for sensor separation and sensor path length (Moore 1986), and the Webb–Pearman–Leuning correction (Webb et al. 1980). To minimize calculation error, half-hour flux data were rejected if one of the following criteria was met: (1) incomplete half-hour measurements mainly caused by a power failure, (2) rain events, and (3) statistical outliers outside the ± 5 standard deviation range of a 10-day running mean window. Approximately 30–45% of flux data were eliminated by the screening criteria, which caused data gaps consistent with other systems (Xu and Baldocchi

2004; Wohlfahrt et al. 2008). Gaps in the diurnal ET record were filled with the mean ET taken over the surrounding 14 days at the same time of the day (Kochendorfer et al. 2011).

Chamber measurements

Within the footprint area of the EC tower and in a southeasterly direction, plots were installed for water fluxes of the shrub and herbaceous layers measurements during the 2014 growing season (May–October). Two treatments were applied: control (C), where the fluxes were measured on undisturbed, and separated (S), where above- and below-ground fluxes were experimentally separated. There were 8 and 16 replicate plots of two treatments for the shrub and herbaceous layers. For the shrub layer measurements, eight healthy plants with an average canopy size were randomly selected (resulting in four plots for C and four for S treatment). At each shrub plot, a stainless steel collar (2 m × 2 m) was inserted into the soil (15-cm depth) to provide a permanent measurement plot. Plastic sheeting (2 m × 3 m) was used to separate the above- and below-ground fluxes during the measurement period. In the center of the sheet, the plastic was sealed around the trunk with sealant. In between measurements, the plastic was folded loosely around the trunk.

For the herbaceous layer, 1 day before the start of each experimental measurement, 16 herbaceous plots with stainless steel collars (0.5 m × 0.5 m) (eight for C and eight for S treatment) were installed 15 cm deep in the soil. At the same time, in the S plots, plant above-ground components were cut off in order to separate plant above- and below-ground components.

Gas exchange measurements were made at 5-day intervals during the 2014 growing season, and each measurement period lasted approximately 24 h: from 07:00 a.m. to 06:00 a.m. the next day. A custom-made transparent polycarbonate chamber (length × width × height: shrub, 2 m × 2 m × 2 m; and herb, 0.5 m × 0.5 m × 0.3 m) was sealed on the previously inserted collar, and H_2O fluxes inside the chamber were measured with the attached infrared gas analyzer (Li-840, LI-COR Inc.). Two electric fans were installed in the chamber to maintain steady temperatures (± 0.5 °C compared to ambient temperature) and humidity during measurement. Water flux under natural radiation was taken at 10-s intervals during a 120-s period (usually starting < 40 s after the equipment was attached).

During the daytime, transparent chamber measurements in C plots directly obtained ET_{shrub} and ET_{herb} values. In S plots, they produced T_{shrub} data for the shrubs, T_{herb} were obtained with difference between C and S plots in herbaceous layer. The water fluxes (F) were calculated using the following equation:

$$F = \frac{P_0 \times V}{R \times S \times (Ta + 273.15)} \times \frac{dC}{dt} \quad (1)$$

where F is the H_2O (mmol H_2O m^{-2} s^{-1}) exchange rate, V is the volume of the chamber, P_0 is the initial pressure, R is the universal gas constant (8.3145 J mol^{-1} K^{-1}), S is the inner surface area of the chamber base, T_a is the mean air temperature in the chamber during measurement, and dC/dt is the slope of the least squares linear regression of H_2O concentration against time. Fluxes were accepted when there was a significant correlation between H_2O concentration and enclosure time ($R^2 > 0.95$, $P < 0.05$).

Bare-soil evaporation

Bare-soil evaporation (E) was measured throughout the growing season by micro-lysimeters in 2014. Cylinders made of PVC with an inner diameter of 15.6 cm and height of 15.2 cm. Every day during the growing season, 20 cylinders were randomly pushed into soil (including beneath shrubs and interplant spaces), the soil-filled cylinder was then removed, cleaned, sealed with a rubber belt to make it water-tight, weighed, and returned to its original location. We weighed the cylinder again after 24 h, and calculated daily bare-soil E as the difference between the two weights.

Oxygen stable isotope measurements

Oxygen stable isotope measurements were used to determine the seasonal water use strategy of dominant shrubs (*H. ammodendron*). Four healthy *H. ammodendron* plants with average canopy size were randomly selected. During May–October, one suberized twig from each plant was sampled in the middle of each month for xylem water. Cut twigs were quickly decorticated and placed into screw-cap glass vials sealed by Parafilm and stored in a freezer for xylem water extraction and isotopic analysis. At the same time, soil samples were collected adjacent to sampled plants. Soil samples were collected at 10-, 20-, and 40-cm intervals

from 0- to 20-, 20- to 100-, and 100- to 400-cm depths, respectively. Four replicates for each layer were sampled and sealed in glass vials and frozen for soil water extraction and isotopic analysis. Every month, groundwater samples were collected from a nearby well. After each rain event (> 2 mm), water samples were collected. Upon collection, water samples were sealed and stored in a freezer for analysis.

Xylem water and soil water were extracted using a cryogenic vacuum distillation extraction line and the extracted water was stored in sealed glass vials at 2 °C. The oxygen isotopic composition of the water was determined by a liquid water isotope analyzer (Eq. 2) (LWIA, DLT-100, Los Gatos Research Inc., Mountain View, CA, USA). The $\delta^{18}O$ values of the xylem water were corrected following Schultz et al. (2011) to eliminate the effect of methanol and ethanol contamination.

$$\delta^{18}O = \left(\frac{R_{sample}}{R_{standard}-1}\right) \times 1000\% \quad (2)$$

where R_{sample} and $R_{standard}$ are the oxygen stable isotopic composition ($^{18}O/^{16}O$ molar ratio) of the sample and the standard water (Standard Mean Ocean Water, SMOW), respectively.

The isotopic values of xylem water were compared with the potential water sources using the IsoSource model (Phillips and Gregg 2003) (http://www.epa.gov/wed/pages/models/stableIsotops/isosource/isosource.htm). For each sample time, we calculated the mean and possible range of water utilization. Source increment was defined as 1% and mass balance tolerance was defined as 0.1 ‰. For details, see Dai et al. (2015).

Investigation of plant cover

Plant cover was determined between 1 May and 31 August at 2-week intervals during the 2014 growing season. To investigate the shrub layer cover, 24 main plots of 20 m × 20 m were randomly established. The widths of all shrub crowns were measured in east–west and north–south directions, and shrub cover was calculated, assuming an elliptical coverage. At the same time, three sub-plots (each 1 m × 1 m) across the diagonal within each main plot were chosen to estimate the herbaceous layer cover using the point intercept method (Kershaw and Looney 1983). The number of points that intercepted a part of a plant were counted and expressed as a percentage of the total number of points recorded per plot (i.e., 100).

Up-scaling water flux

Simple area-weighted up-scaled models were established to upscale the fluxes measured by the lysimeters and chamber methods and to quantify the ecosystem scale water fluxes contributed by the shrub and herbaceous layers. Based on the established plant cover of the different layers, the following area-weighted models (Eqs. 3–5) were used at the beginning (B), middle (M), and end (E) of the growing season, respectively:

$$F_B = 0.45F_{shrub} + 0.37F_{herb} + 0.18F_{soil} \quad (3)$$

$$F_M = 0.43F_{shrub} + 0.11F_{herb} + 0.46F_{soil} \quad (4)$$

$$F_E = 0.38F_{shrub} + 0.04F_{herb} + 0.52F_{soil} \quad (5)$$

Determining water balance

The water balance of the study area over a period of time can be expressed as follows:

$$PPT + GW = ET + R + D + \Delta W \quad (6)$$

where PPT is precipitation, GW the contribution from groundwater, R is surface runoff, D is deep drainage and W is the change in water storage within the soil layer. R and D can be neglected as the study site is flat and precipitation was not intense. The high evaporative demand and discontinuous rain pulse events result in little or no soil water storage change on annual scales. Therefore, the contributions of groundwater to ET can be defined of difference between ET and precipitation.

Statistical analyses

All descriptive statistics (mean and standard errors, SE) and statistical analyses (including linear regression, one-way and two-way ANOVA) were performed with the SPSS 13.0 statistical package (SPSS Inc., Chicago, IL, USA). The significant level was set to 0.05. Partial least square (PLS) regression analysis (Geladi and Kowalski 1986) was conducted to investigate the model

component structure among the major drivers—independent variables including various measures of R_n, PPT, temperature, vapor pressure deficit (VPD), SWC, plant cover, and soil cover—explaining the seasonal variations of T_{shrub}, T_{herb}, and E (dependent variables). All means for variables are averaged for 30-day periods; except PPT which was the total for 30-day periods. The PLS regression analysis was carried out using SIMCA software v. 11.5 (UMETRICS, Umea, Sweden), which includes four steps: data normalization (Z-score normalization method), multiple correlation information and system nose elimination, main factors determination, and PLS regression model establishment. The Origin 8.0 software package (Origin Lab Ltd., Guangzhou, China) was used for graphical output.

Results

Meteorological conditions and ecosystem ET

The seasonal variations in the major meteorological conditions and ET in 2014 were presented in Fig. 1. The seasonal trends of the daily average R_n and T_a were similar, with minimum values (−2 to −11 W m^{-2}) in winter and maximum values (119 to 146 W m^{-2}) in summer. The daily maximum and minimum T_a was within 24–30 °C and −12 to −21 °C (Fig. 1a, b). Annual precipitation was 108 mm, 55 mm below the long-term average of 163 mm for 1985–2010. Seasonal variation in water table depth was small, with the minimum of 3.4 m in spring and early summer, and the maximum of 4.2 m in other periods (Fig. 1d). ET showed a seasonal trend with daily higher rates at the beginning of the growing season (1.97 mm day^{-1}). In winter, when T_a was below freezing, plants were dormant or senescent and ET decrease near zero (Fig. 1c).

Cross-validation of methods and partitioning ET components

Shrub and herbaceous layer T (T_{shrub} and T_{herb}) and bare-soil E measured by the chamber and microlysimeters were up-scaled to ecosystem ET using simple area-weighted models (Eqs. 3–5) and these were compared with the ET measured by EC (Fig. 2a). The result demonstrated that these methods cross-validated very well, with a significant linear relationship ($R^2 > 0.89$, $P < 0.05$) (Fig. 2a). The seasonal pattern of ET components differed significantly ($F = 10.87$, $P < 0.05$), and average E, T_{shrub}, and T_{herb} also differed significantly ($F = 39.93$, $P < 0.05$). Bare-soil E reached a maximum (0.69 mm day^{-1}) at the beginning of the growing season, and decreased to nearly zero at the end of the growing season (Fig. 2b). The seasonal patterns between T_{shrub} and T_{herb} differed markedly (Fig. 2c, d). The maximum daily T_{herb} was 0.55 mm day^{-1} after spring snowmelt period around day of year 120, and decreased thereafter till the middle and the end of the growing season (Fig. 2c). T_{shrub} showed a different trend: at the beginning of the growing season, it gradually increased, reached a maximum value of 1.84 mm day^{-1}, remained stable

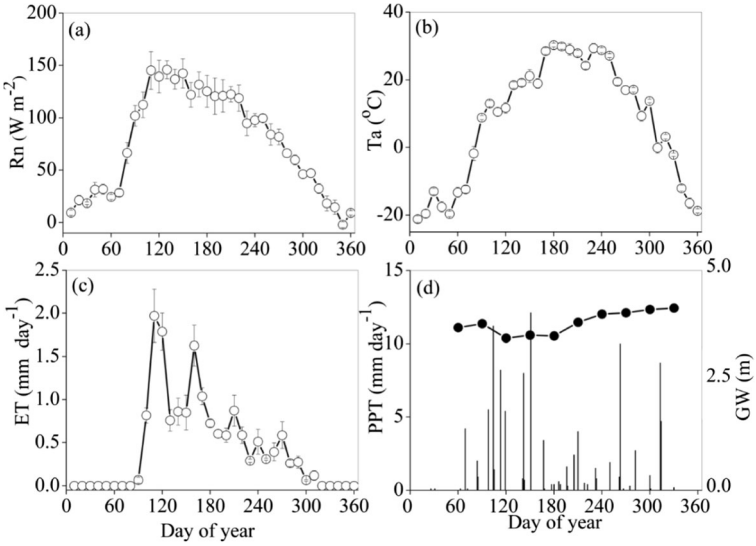

Fig. 1 Seasonal variations in net radiation (R_n) (**a**), air temperature (T_a) (**b**), evapotranspiration (ET) (**c**), precipitation (PPT), and groundwater table depth (GW) (**d**) at the study site during 2014. For R_n, T_a, and ET, symbols represent the mean ± SE for 10-day periods

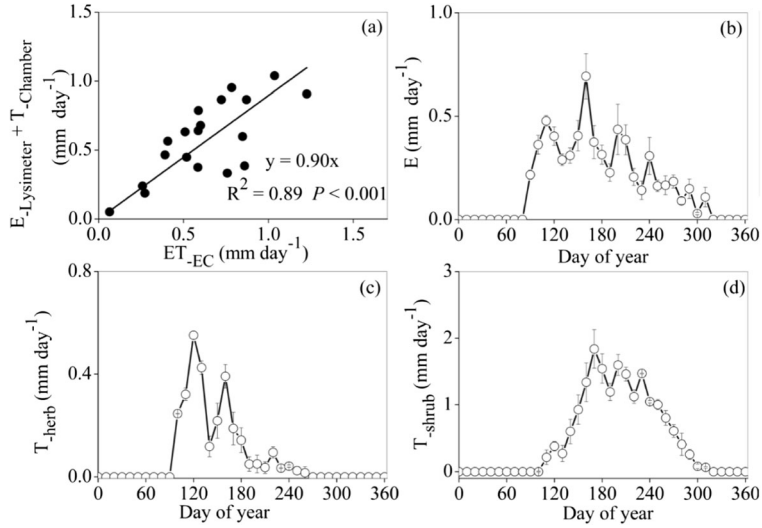

Fig. 2 Relationship for daily evapotranspiration (ET) between eddy covariance (ET_{-EC}) and chamber and micro-lysimeters ($E_{-Lysimeter}$ + $T_{-chamber}$) (**a**), seasonal variations of bare-soil evaporation (E) (**b**), transpiration of the herbaceous (T_{herb}), (**c**) and shrub (T_{shrub}) (**d**) layers during the growing season. Statistically significant linear relationships at $P < 0.05$. Symbols in **b**–**d** represent the mean ± SE for 10-day periods

around 1.2 mm day^{-1} during the middle, then decreased to zero at the end of the growing season (Fig. 2d).

Quantification of the seasonal variations in T_{shrub}/ET, T_{herb}/ET, and E/ET had been given in Fig. 3. The seasonal variation of T/ET differed among the shrub and herbaceous layers. In the shrub layer, T_{shrub}/ET exhibited an increasing trend and reached its peak value around July, with a range of 30–84% (Fig. 3a). In contrast, T_{herb}/ET showed a decreasing trend, reached a maximum in May with 33%; it then decreased gradually, reaching near zero in early of August (Fig. 3b). Seasonal variation in E/ET was relatively stable, with range of 15–57% (Fig. 3c). Average T_{shrub}/ET, T_{herb}/ET, and E/ET differed significantly throughout the growing season, ($F = 12.48$, $P < 0.05$). In total, T_{shrub}, T_{herb}, and E were 70, 16, and 82 mm year^{-1}, and they account for 42, 9, and 49% of total ET, during 2014 (Fig. 3d).

The contribution of groundwater to ET components

In the growing season, the $\delta^{18}O$ values of precipitation, groundwater and xylem water were showed in Fig. 4. The $\delta^{18}O$ values of precipitation ranged from −12.3 to 0.2 ‰ during the growing season, with the average value of -4.8 ± 1.2 ‰ (Fig. 4a). The small seasonal changes in the $\delta^{18}O$ values of xylem water mirrored those seen in the groundwater with the values around -9.9 ± 0.1 ‰ (Fig. 4b).

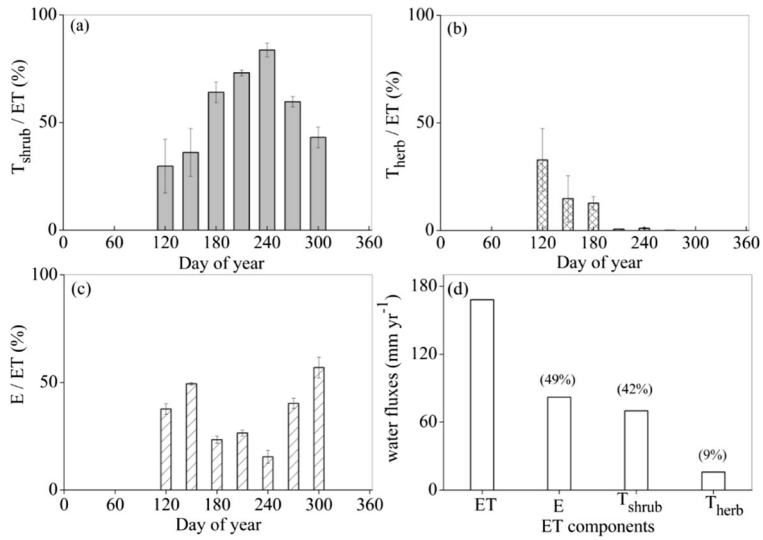

Fig. 3 Seasonal variations in T_{shrub}/ET (**a**), T_{herb}/ET (**b**), and E/ET (**c**), and total ET, E, T_{shrub}, and T_{herb} (**d**) at the study site during 2014. The value in bracket represents the percentage of E/ET, T_{shrub}/ET, and T_{herb}/ET, respectively. Symbols in **a**–**c** represent the mean ± SE for 30-day periods

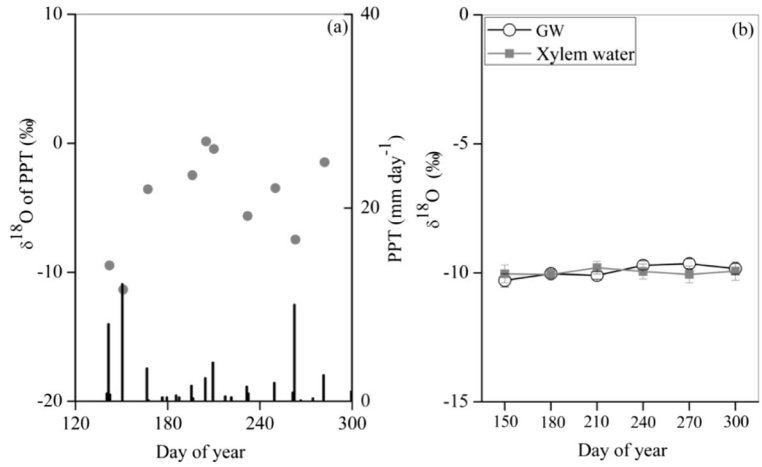

Fig. 4 Seasonal variation of the $\delta^{18}O$ values of precipitation (PPT) (**a**), groundwater (GW) and xylem water (**b**) during the growing season. Error bars represent SEs of mean $\delta^{18}O$ values ($n = 4$)

The IsoSource model was used to determine water-use strategy of *H. ammodendron* shrubs and showed that they exhibited a stable trend in water use during the growing season (Fig. 5a). During May–October, *H. ammodendron* use similar water source: greater than 85% ± 5% (range 86–98%) of the xylem water was derived from groundwater, with the possible ranges of soil water less than 9% ± 6% (Fig. 5a). This partitioning of water sources was rather stable from month to month, without significant variance throughout the growing season ($P > 0.05$).

Combining the data obtained from T_{shrub} with the chamber measurements allowed quantification of the contribution of groundwater to T_{shrub}. Seasonal variation in groundwater contribution to T_{shrub} showed a single-peak pattern, with the maximum in June (1.42 ± 0.13 mm day^{-1}), then decreased gradually until the minimum of 0.24 ± 0.09 mm day^{-1} in October (Fig. 5b). In addition, there was no significant linear relationship between groundwater supply and T_{shrub} ($R^2 = 0.50$, $P = 0.12$) (Fig. 5, data not shown).

The major drivers of seasonal variations in ET components

The main factors and regression coefficients were determined by principal components analysis (PCA) and canonical correlation analysis (CCA) in PLS regression process (Fig. 6). Components were determined by cross-validation. The results showed that T_{shrub} had one component; it can explain and predict 80 and 72% of T_{shrub} (Fig. 6a). T_{herb} and E had two components; they can

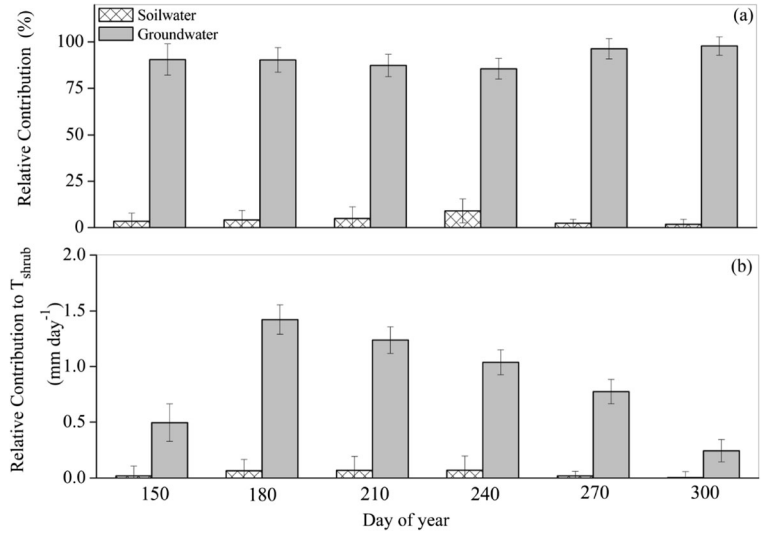

Fig. 5 Seasonal changes in relative contribution of potential water resources for *H. ammodendron* shrubs (**a**) and groundwater and soil water contributions to shrub transpiration (T_{shrub}) (**b**) during the growing season. **a** Column heights represent the mean value of relative contributions and bars represent the ranges of minimum/maximum, both were calculated using the IsoSource model. **b** Symbols in represent the mean ± SE for 30-day periods

explain and predict T_{herb} and E at more than 90 and 70% (Fig. 6b, c). Combining CCA regression models, we found T_{air} was the main driver of T_{shrub}, SWC and herbaceous plant cover were the main drivers of T_{herb}, and R_n and PPT were the main drivers of E (Fig. 6). Using the PLS regression models, the comparison of observed and predicted ET components showed that there were significant linear relationship between observed and predicted values (T_{shrub}: $R^2 = 0.79$, T_{herb}: $R^2 = 0.96$, E: $R^2 = 0.89$, $P < 0.05$) (Fig. 7).

Discussion

Partitioning source and sinking process of ET is important to accurately assess water balance in water-limited ecosystems. Using diverse methods including EC, static chambers, micro-lysimeters, and oxygen stable isotope measurements, we partitioned ET into T_{shrub}, T_{herb}, and E, quantified the contribution of groundwater to ET components, and found the main drivers of ET components (summarized in Fig. 7). Our results provide quantitative evidence for previous hypotheses that seasonal patterns and main drivers of ET components differ among each other, and groundwater uptake by phreatophytes is a relevant part to the total water balance in these desert ecosystems. Our chamber measurements were conducted during a relatively dry year (108 mm precipitation), compared to the multi-year average precipitation of 163 mm at the study site (Huang and Li 2015; Liu et al. 2016). However, this did not affect our verification of the two hypotheses, as shrub plants depend on groundwater as their primary water source, and the stable snow cover is the key determinant to the germination and rapid growth of herbaceous plants (Fan et al. 2013; Dai et al. 2015; Huang and Li 2015).

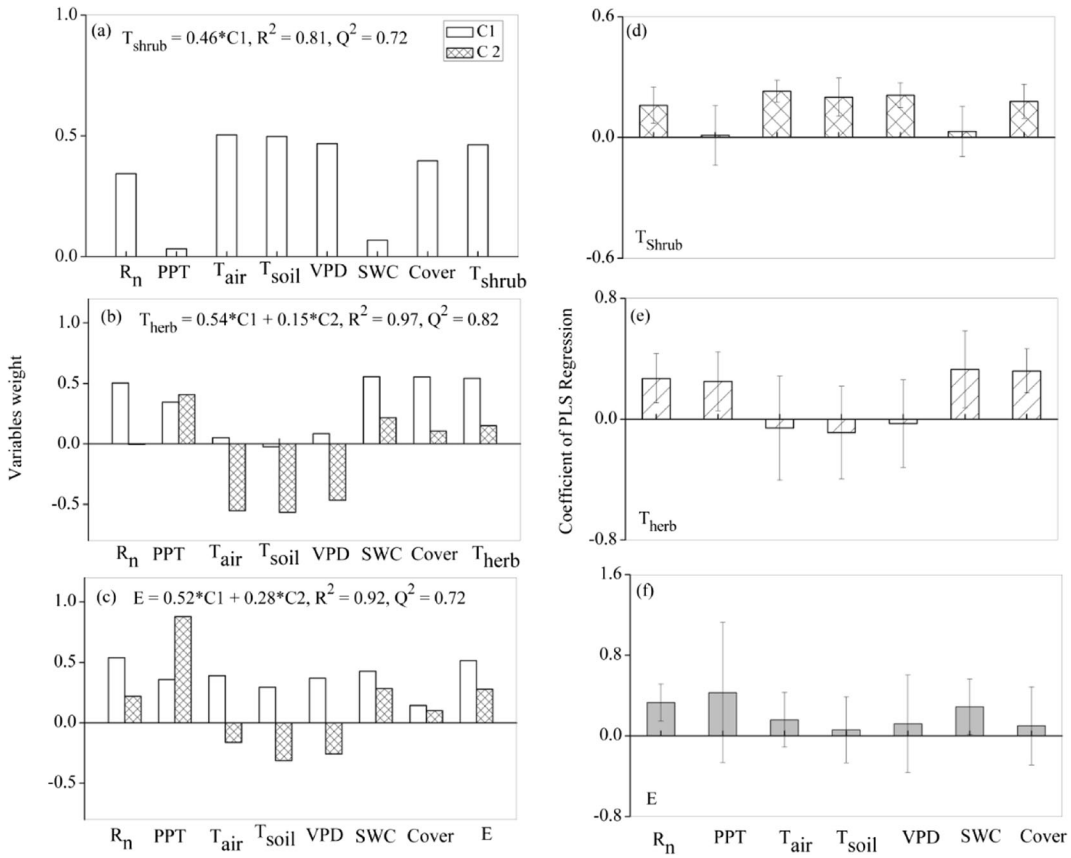

Fig. 6 Determining the main factors (**a**–**c**) and regression coefficients in PLS Regression process. T_{shrub}: shrub layer transpiration, T_{herb}: herbaceous layer transpiration, E: bare-soil evaporation, R_n: net radiation, PPT: precipitation, T_a: air temperature, T_{soil}: soil temperature, VPD: vapor pressure deficit, SWC: soil water content. All means for variables are averaged for 30-day periods; except PPT which is the total for 30-day periods. "C" represents component. R^2 represents the fraction of explanation of T_{shrub}, T_{herb}, and E by the components, Q^2 represents the fraction of prediction of T_{shrub}, T_{herb}, and E by the components

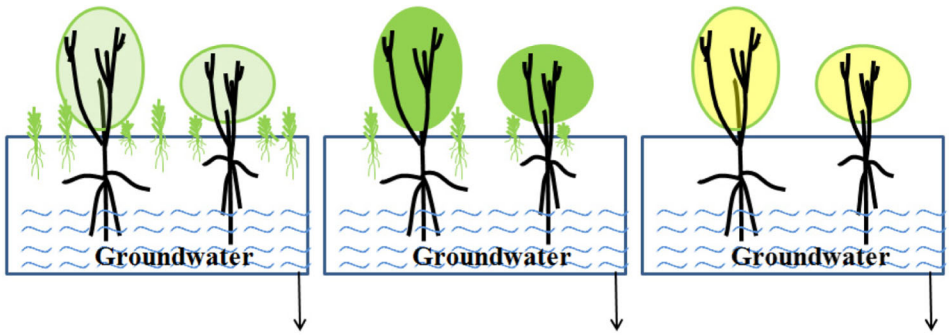

GS	Spring (May-Jun)	Summer (Jul-Aug)	Autumn (Sept-Oct)
Dominated plant	Shrubs, spring annuals	Shrubs, summer annuals and perennials	Shrubs
Water resources	Groundwater and precipitation	Groundwater and precipitation	Groundwater
The sources of ET	T_{shrub}: 70 mm (42%), T_{herb}: 16 mm (9%), E: 82 mm (49%)		
The contribution of GW to ET	ET: 60 mm (36% of total ET), T_{shrub}: 51 mm (73% of T_{shrub})		
PLS Regression Models	$T_{shrub} = 0.16R_n + 0.01PPT + 0.23T_a + 0.20T_{soil} + 0.21VPD + 0.03SWC + 0.18$Plant cover ($R^2 = 0.79$)		
	$T_{herb} = 0.27R_n + 0.25PPT - 0.06T_a - 0.09T_{soil} - 0.03VPD + 0.33SWC + 0.32$Plant cover ($R^2 = 0.96$)		
	$E = 0.33R_n + 0.43PPT + 0.16T_a + 0.06T_{soil} + 0.12VPD + 0.29SWC + 0.10$Soil cover ($R^2 = 0.89$)		

Fig. 7 Conceptual diagram illustrating the dominant plant type, water resource, the sources and sinking process of ET, and PLS regression models for shrub layer transpiration (T_{shrub}), herbaceous layer transpiration (T_{herb}), and bare-soil evaporation (E). Different colors in shrub crowns indicate different growing stages (light green is start, green is middle, and yellow is end)

Therefore, our conclusions are representative of the desert ecosystems, which have two stable water sources: groundwater and snow melted water.

Seasonal variations in ET components

Our study used combined methods to show that the T_{shrub} and T_{herb} differed markedly in seasonal variation (Figs. 2 and 3). The different water-use strategies by the shrub and herbaceous layers probably had considerable effects on the unequal seasonal patterns of T_{shrub} and T_{herb} throughout the growing season. The shrub layer was dominated by phreatophytes that depend on groundwater as their main water source (Figs. 4 and 5), which results in no-water-limited, non-rainfall-dependent physiological activity (photosynthesis and transpiration) throughout the hot and dry parts of the season (Paço et al. 2009; Scott et al. 2014). In contrast, the herbaceous layer employs different water-use strategies through the growing season. The beginning of the season combines sufficient soil water availability (snowmelt water and spring precipitation) with increasing temperatures, which allows spring annuals to grow at surprisingly fast rates. This causes higher transpiration between May and the mid-June (Fan et al. 2013; Huang and Li 2015). After the spring annuals die, other slower growing herbaceous components take over (summer annuals and perennials), and they often depend on small summer rain events (< 5 mm) of short duration to survive. Such periods of lower T_{herb} can be explained in two ways. First, small rain events cannot reach plant roots and return to the atmosphere by soil E (Huxman et al. 2004). Second, drought events can lead to plant senescence or damage to cell organs, and reduce plant water-use efficiency (Smith et al. 1997).

The contribution of groundwater to ET components

Groundwater is a major water resource of ET in water-limited ecosystems (Fitzpatrick et al. 2001; Liu et al. 2012). However, groundwater resource is often underestimated, because T_{shrub} from roots tapping the

water table is not taken into account (Favreau et al. 2009; Miller et al. 2010; Balugani et al. 2017). Our results showed that for the shrub layer, greater than 85% (range of 86–98%) of xylem water was derived from groundwater. Most of the groundwater was consumed by T_{shrub} (51 mm year^{-1}), accounted for 73% of T_{shrub}. The contribution of groundwater to ET was 60 mm year^{-1}, represented more than 35% of total ET during 2014. The high T_{shrub} values are not surprising, since deep-rooted plants in water-limited ecosystem often rely on deep rooting and on the ability to tap water from permanent water tables (Walter 1973; Jackson et al. 1996; Balugani et al. 2017). These results are consistent with reports from other water-limited ecosystems. For example, Miller et al. (2010), using the water table fluctuation method in an oak savanna in the western Sierra Nevada foothills, found groundwater uptake rates of 4–25 mm month^{-1} that accounted for up to 80% of total ET. David et al. (2007) used stable isotope analyses in xylem water, soil water, and groundwater in Mediterranean evergreen oak woodlands of southern Portugal to show that groundwater withdrawal accounted for more than 70% of total tree *T*. As such, groundwater contributions to ET are important and may represent a large proportion of total ET, at least in water-limited ecosystems.

The major drivers of ET components

The seasonal variations of ET components were shaped by different factors (Fig. 6). The shrub layer was dominated by deep-rooted plants (phreatophytes), and T_{shrub} was not restricted by water conditions, such as precipitation and SWC (Smith et al. 1997; Liu et al. 2017). Instead, an increase in T_a is expected to increase plant water use. At low to moderate levels of T_a, the decrease in stomatal conductance is typically not large enough to prevent increased T_{shrub} (Leuning 1995; Hasper et al. 2016). The herbaceous layer was dominated by shallow-rooted species that use precipitation as the main water source, and T_{herb} is more sensitive to water availability (Hu et al. 2009; Liu et al. 2012). Additionally, increases in shallow-rooted plant cover may reduce bare-soil E and thus increase T_{herb} (Liu et al. 2012, 2016). These mechanisms may explain the different drivers of ET components, and may be an important source of uncertainty in predictions of water cycling under projected climatic change scenarios.

Study limitation and conclusions

Our study aims at a better understanding of source and sinking process of ET for a groundwater-dependent desert plant community. Constrained by experimental design, partition sinking process of ET is still incomplete; the water resource of E and T_{herb} would not separately distinguish between groundwater and precipitation. To solve this problem, a more focused study on identifying groundwater *E* and soil *E* of water from precipitation is required. Nevertheless, the results still confirmed that seasonal patterns and main drivers of ET components differed among each other, and indicated that the whole plant community cannot be considered as a single, spatially uniform system for water vapor exchange with the atmosphere. The results emphasized again, in groundwater-dependent desert plant community with phreatophytes, the often neglected groundwater is a relevant contribution to ET, and most of the groundwater is consumed by *T* of phreatophytes. Overall, it is critical to define accurately the source and sinking process of ET; such fundamental understanding is required not only to improve surface-atmosphere models but also to better budget and manage the water resource in water-limited ecosystems.

Acknowledgements We thank all staff of the Fukang Station of Desert Ecology for their excellent field and laboratory assistance.

Funding information Financial support was provided by the Xinjiang Province Key Science and Technology projects (2016A03008-4-5), The National Natural Science Foundation of China (41771121, 41730638), Key Research Program of Frontier Sciences of Chinese Academy of Sciences (QYZDJ - SSW - DQC014), and Youth Innovation Promotion Association of Chinese Academy of Sciences (2017476).

References

Anderson M, Norman J, Kustas W, Houborg R, Starks P, Agam N (2008) A thermal-based remote sensing technique for routine mapping of land-surface carbon, water and energy fluxes from field to regional scales. Remote Sens Environ 112(12):4227–4241

Austin AT, Yahdjian L, Stark JM, Belnap J, Porporato A, Norton U, Ravetta DA, Schaeffer SM (2004) Water pulses and biogeochemical cycles in arid and semiarid ecosystems. Oecologia 141(2):221–235

Baldocchi DD, Xu L (2007) What limits evaporation from Mediterranean oak woodlands—the supply of moisture in the soil, physiological control by plants or the demand by the atmosphere? Adv Water Resour 30:2113–2122

Balugani E, Lubczynski MW, Reyes-Acosta L, van der Tol C, Frances AP, Metselaar K (2017) Groundwater and unsaturated zone evaporation and transpiration in a semi-arid open woodland. J Hydrol 547:54–66

Barbeta A, Penuelas J (2017) Relative contribution of groundwater to plant transpiration estimated with stable isotopes. Sci Rep 7:10580

Bertram J, Dewar RC (2013) Statistical patterns in tropical tree cover explained by the different water demand of individual trees and grasses. Ecology 94:2138–2144

Connor S, Nelson PN, Armour JD, Hénault C (2013) Hydrology of a forested riparian zone in an agricultural landscape of the humid tropics. Agric Ecosyst Environ 180:111–122

Dai Y, Zheng XJ, Tang LS, Li Y (2015) Stable oxygen isotopes reveal distinct water use patterns of two Haloxylom species in the Gurbantonggut Desert. Plant Soil 389:73–87

David TS, Henriques MO, Kurz-Besson C, Nunes J, Valente F, Vaz M, Pereira JS, Siegwolf R, Chaves MM, Gazarini LC, David JS (2007) Water-use strategies in two co-occurring Mediterranean evergreen oaks: surviving the summer drought. Tree Physiol 27:793–803

De Arruda PHZ, Vourlitis GL, Santanna FB, Pinto OB, Lobo FD, Nogueira JD (2016) Large net CO_2 loss from a grass-dominated tropical savanna in south-central Brazil in response to seasonal and interannual drought. J Geophys Res 121:2110–2124

Elmore AJ, Manning SJ, Mustard JF, Craine JM (2006) Decline in alkali meadow vegetation cover in California: the effects of groundwater extraction and drought. J Appl Ecol 43:770–779

Emus D, Zolfaghar S, Villalobos-Vega R, Cleverly J, Huete A (2015) Groundwater-dependent ecosystem: recent insights from satellite and field-based studies. Hydrol Earth Syst Sci 19:4229–4256

Fahle M, Dietrich O (2014) Estimation of evapotranspiration using diurnal groundwater level fluctuations: comparison of different approaches with groundwater lysimeter data. Water Resour Res 50:273–286

Fan LL, Tang LS, Wu LF, Ma J, Li Y (2013) The limited role of snow water in the growth and development of ephemeral plants in a cold desert. J Veg Sci 25:681–690

Favreau G, Cappelaere B, Massuel S, Leblanc M, Boucher M, Boulain N, Leduc C (2009) Land clearing, climate variability, and water resources increase in semiarid southwest Niger: a review. Water Resour Res 45(7)

Fitzpatrick RW, Rengasamy P, Merry RH, Cox JW (2001) Is dryland soil salinisation reversible? The National Dryland Salinity Program. http://www.ndsp.gov.au

Geladi P, Kowalski BR (1986) Partial least-squares regression: a tutorial. Anal Chim Acta 185:1–17

Hasper TB, Wallin G, Lamba S, Hall M, Jaramillo F, Laudon H, Linder S, Medhurst JL, Rantfors M, Sigurdsson BD, Uddling J (2016) Water use by Swedish boreal forests in a changing climate. Fun Ecol 30:690–699

Hu ZM, Yu GR, Zhou YL, Sun XM, Li YN, Shi PL, Wang YF, Song X, Zheng ZM, Zhang L, Li SG (2009) Partitioning of evapotranspiration and its controls in four grassland ecosystems: application of a two-source model. Agric For Meteorol 149:1410–1420

Huang G, Li Y (2015) Phenological transition dictates the seasonal dynamics of ecosystem carbon exchange in a desert steppe. J Veg Sci 26(2):337–347

Huxman TE, Snyder KA, Tissue D, Leffler AJ, Ogle K, Pockman WT, Sandquist DR, Potts DL, Schwinning S (2004) Precipitation pulses and carbon fluxes in semiarid and arid ecosystems. Oecologia 141:254–268

Huxman TE, Wilcox BP, Breshears DD, Scott RL, Snyder KA, Small EE, Hul-tine K, Pockman WT, Jackson RB (2005) Ecohydrological implications of woody plant encroachment. Ecology 86:308–319

Jackson RB, Canadell J, Ehleringer JR, Mooney HA, Sala OE, Schulze ED (1996) A global analysis of root distributions for terrestrial biomes. Oecologia 108:389–411

Jasechko S, Sharp ZD, Gibson JJ, Birks SJ, Yi Y, Fawcett PJ (2013) Terrestrial water fluxes dominated by transpiration. Nature 496:347–350

Joffre R, Rambal S (1993) How tree cover influences the water balance of Mediterranean rangelands. Ecology 74:570–582

Kershaw KA, Looney JH (1983) Quantitative and dynamic plant ecology. Edward Arnold, London

Kochendorfer J, Castillo EG, Haas E, Oechel WC, Paw KT (2011) Net ecosystem exchange, evapotranspiration and canopy conductance in a riparian forest. Agric For Meteorol 151: 544–553

Kool D, Agam N, Lazarovitch N, Heitman JL, Sauer TJ, Ben-Gal A (2014) A review of approaches for evapotranspiration partitioning. Agric For Meteorol 184:56–70

Law BE, Falge E, Gu L, Baldocchi DD, Bakwin P, Berbigier P, Davis K, Dolman AJ, Falk M, Fuentes JD, Goldstein A, Granier A, Grelle A, Hollinger D, Janssens IA, Jarvis P, Jensen NO, Katul G, Mahli Y, Matteucci G, Meyers T, Monson R, Munger W, Oechel W, Olson R, Pilegaard K, Paw KT, Thorgeirsson H, Valentini R, Verma S, Vesala T, Wilson K, Wofsy S (2002) Environmental controls over carbon dioxide and water vapor exchange of terrestrial vegetation. Agric For Meteorol 113:97–120

Leuning R (1995) A critical appraisal of a combined stomatal-photosynthesis model for C-3 plants. Plant Cell Environ 18: 339–355

Li J, Yu B, Zhao CY, Nowak RS, Zhao Z, Sheng Y, Li J (2013) Physiological and morphological responses of Tamarix ramosissima and Populus euphratica to altered groundwater availability. Tree Physiol 33:57–68

Liu R, Pan LP, Jenerette GD, Wang QX, Cieraad E, Li Y (2012) High efficiency in water use and carbon gain in a wet year for a desert halophyte community. Agric For Meteorol 162-163: 127–135

Liu R, Cieraad E, Li Y, Ma J (2016) Precipitation pattern determines the inter-annual variation of herbaceous layer and carbon fluxes in a phreatophyte-dominated desert ecosystem. Ecosystems 19:601–614

Liu B, Guan HD, Zhao WZ, Yang YT, Li SB (2017) Groundwater facilitated water-use efficiency along a gradient of groundwater depth in arid northwestern China. Agric For Meteorol 233:235–241

Lloyd J, Bird MI, Vellen L, Miranda AC, Veenendaal EM, Djagbletey G, Miranda HS, Cook G, Farquhar GD (2008) Contributions of wood and herbaceous vegetation to tropical savanna ecosystem productivity: a quasi-global estimate. Tree Phys 28:451–468

Miller GR, Chen X, Rubin Y, Ma S, Baldocchi DD (2010) Groundwater uptake by woody vegetation in a semiarid oak savanna. Water Resour Res 46(10):W10503

Moore CJ (1986) Frequency response corrections for eddy correlation systems. Bound-Layer Meteorol 37:17–35

Morillas L, Leuning R, Villagarcía L, García M, Serrano-Ortiz P, Domingo F (2013) Improving evapotranspiration estimates in Mediterranean drylands: the role of soil evaporation. Water Resour Res 49:6572–6586

Paço TA, David TS, Henriques MO, Pereira JS, Valente F, Banza J, Pereira FL, Pinto C, David JS (2009) Evapotranspiration from a Mediterranean evergreen oak savannah: the role of trees and pasture. J Hydrol 369(1–2):98–106

Phillips DL, Gregg JW (2003) Source partitioning using stable isotopes: coping with too many sources. Oecologia 136: 261–269

Schlesinger WH, Jasechko S (2014) Transpiration in the global water cycle. Agric For Meteorol 189-190:115–117

Schultz NM, Griffis TJ, Lee XH, Baker JM (2011) Identification and correction of spectral contamination in $^{2}H/^{1}H$ and $^{18}O/^{16}O$ measured in leaf, stem, and soil water. Rapid Commun Mass Spectrom 25:3360–3368

Scott RL, Cable WL, Huxman TE, Nagler PL, Hernandez M, Goodrich DC (2008) Multiyear riparian evapotranspiration and groundwater use for a semiarid watershed. J Arid Environ 72(7):1232–1246

Scott RL, Huxman TE, Barron-Gafford GA, Jenerette GD, Young JM, Hamerlynck EP (2014) When vegetation change alters ecosystem water availability. Glob Change Biol 20:2198–2210

Smith SD, Monson RK, Anderson JA (1997) The physiological ecology of North American desert plants. Springer-Verlag, Berlin, Heidelberg, New York

Sutanto SJ, van den Hurk B, Dirmeyer PA, Seneviratne SI, Rockmann T, Trenberth KE, Blyth EM, Wenninger J, Hoffmann G (2014) HESS opinions "a perspective on isotope versus non-isotope approaches to determine the contribution of transpiration to total evaporation". Hydrol Earth Syst Sci 18(8):2815–2827

Villegas JC, Dominguez F, Barron-Gafford GA, Adams HD, Guardiola-Claramonte M, Sommer ED, Selvey AW, Espeleta JF, Zou CB, Breshears DD, Huxman TE (2015) Sensitivity of regional evapotranspiration partitioning to variation in woody plant cover: insights from experimental dryland tree mosaics. Glob Ecol Biogeogr 24:1040–1048

Vourlitis GL, de Almeida Lobo F, Pinto OB, Zappia A, Dalmagro HJ, De Arruda PHZ, De Souza Nogueira J (2015) Variations in aboveground vegetation structure along a nutrient availability gradient in the Brazilian pantanal. Plant Soil 389:307–321

Walter H (1973) Vegetation of the earth. Springer-Verlag, New York 237p

Wang L, Good SP, Caylor KK (2014) Global synthesis of vegetation control on evapotranspiration partitioning. Geophys Res Lett 41(19):6753–6757

Wang P, Yamanaka T, Li XY, Wei ZW (2015) Partitioning evapotranspiration in a temperate grassland ecosystem: numerical modeling with isotopic tracers. Agric For Meteorol 208:16–31

Webb EK, Pearman GI, Leuning R (1980) Correction of flux measurements for density effects due to heat and water vapor transfer. Q J R Meteorol Soc 106:85–100

Wilczak JM, Oncley SP, Stage SA (2001) Sonic anemometer tilt correction algorithms. Bound-Layer Meteorol 99(1): 127–150

Wohlfahrt G, Fenstermaker LF, Arnone JA (2008) Large annual net ecosystem CO_2 uptake of a Mojave Desert ecosystem. Glob Chang Biol 14:1475–1487

Xu LK, Baldocchi DD (2004) Seasonal variation in carbon dioxide exchange over a Mediterranean annual grassland in California. Agric For Meteorol 1232:79–96

Zhou HF, Zheng XJ, Zhou BJ, Dai Q, Li Y (2012) Sublimation over seasonal snowpack at the southeastern edge of a desert in central Eurasia. Hydrol Process 26:3911–3920